

# A Comparative Study of Tooth Wear, Mechanical Power Losses and Efficiency in Normal and High Contact Ratio Asymmetric Spur Gears

R. Prabhu Sekar \*

*Mechanical Engineering Department, Motilal Nehru National Institute of Technology, Allahabad, India*

Received 12 November 2019; accepted 12 January 2020

## ABSTRACT

The surface tooth wear which occurs at the gear contact region due to inadequate contact strength of the tooth is one of the predominant modes of gear failures. Currently, higher contact ratio spur gears are increasingly used in power transmission applications such as aircraft, wind turbine, automobiles and compact tracked vehicles due to their high load carrying capacity. In this work, the direct design is found to be one of the efficient gear design methods to reduce the tooth surface wear on high contact ratio asymmetric spur gears. Asymmetric gear tooth is defined, as one whose tooth geometry of the drive and coast sides is not symmetric. Asymmetry between tooth sides is achieved by providing two different pressure angles at the respective coast and drive side pitch circles. The area of existence diagrams for normal and high contact ratio gears have been developed to select suitable design solution with the given variables of gear ratio, contact ratio and teeth number. The contact load capacity, wear resistance, power losses and mechanical efficiency have also been deduced for directly designing normal and high contact ratio asymmetric spur gears.

© 2020 IAU, Arak Branch. All rights reserved.

**Keywords :** Asymmetric gear; Direct design; High contact ratio; Power losses; Wear depth.

## 1 INTRODUCTION

**G**EARING is one of the most important structural components in mechanical power transmission systems. The transfer of power from the driver to the driven mainly depends on the number of gear teeth pairs, which come in contact during the mesh cycle. This number of contact pair changes as the gear rotates in and out of mesh. The contact ratio in transverse plane is more than two in high contact ratio (HCR) asymmetric gears (number of contact pairs  $\varepsilon_d > 2$ ) which means that two or three pairs teeth of are in contact during the transmission. However, the actual contact ratio is always less than two ( $1 < \varepsilon < 2$ ) in normal contact ratio (NCR) asymmetric spur gears. Due to the basic advantage of absence of a single pair contact, HCR gears have received more attention for use in heavy load carrying applications such as aircraft, wind turbine and compact tracked vehicles. Elkholy [1] developed an

\*Corresponding author. Tel.: +91 9894986396.  
E-mail address: [prabhusekar.r@gmail.com](mailto:prabhusekar.r@gmail.com) (R. Prabhu Sekar).

analytical relationship to determine the mesh stiffness and tooth load in high contact ratio gears. Haung Tsai and Chein Tsai [2] developed a method of designing higher contact ratio symmetric spur gear using quadratic parametric tooth profiles for stub tooth system and with undercut free contact. They demonstrated that the tooth root stresses and the static transmission errors were always less in the high contact ratio gears. The mesh compliance and tooth deflection were determined in normal contact ratio symmetric spur gear using finite element tooth contact analysis by Arafa and Megahad [3]. They reported that the tooth deflection was largely dependent on the load position along the involute tooth profile. The conjugate meshing face gear were implemented to high shaft angle intersecting axis gears by Saribay [4]. The fillet stress in the face gear was approximately 6% less than the same size of the spur gear. Wang and Howard [5] investigated the effect of different input loads on load share, tooth bending stress and contact stress in HCR gears using finite element method. Increment of addendum height increased the contact ratio (from NCR to HCR) which lead to considerable reduction tooth contact and bending stresses [6]. The load sharing ratio along the path of contact in HCR symmetric spur gears was determined from the minimum elastic potential criterion by Pedrero et al. [7]. It was found from their work that the maximum load sharing ratio in HCR gears was 0.6 (60% of total normal load), whereas it was one (100% of total normal load) in NCR spur gears. The finite element model for HCR gears was developed and the bending stress analysis was carried out by Bansan et al. [8]. Their findings showed that the highest bending stress developed at the critical root region, when the teeth contact pair made contact at the second lowest point of double tooth contact in HCR gears. For the given torque, the life of the HCR gear was higher (double times) than NCR gear which was mainly due to subject lower loads [9]. The contact and fillet stresses that developed in HCR symmetric spur gears were comparatively lower than that of NCR spur gears [10].

Many papers discussed the tooth wear prediction methodologies with improved wear models for predicting the tooth wear on standard and non-standard symmetric spur gears. Archard [11] developed a common relation to calculate the sliding wear between the pinion and gear teeth surfaces. In metallic gears, wear depth depends on tooth load, contact pressure, elasto hydrodynamic lubrication thickness, coefficient of friction and sliding distance between the contact pair. The rate of wear along the path of contact was determined through a derived analytical expression by Wu and Cheng [12]. Results showed that the maximum amount of material removed from the flank region (dedendum portion) was higher than that of face region of the driving gear. Flodin and Anderson [13] proposed a wear estimation methodology for calculating the sliding wear in symmetric spur gears using Archard's wear equations. The influence of contact pressure on tooth surface wear was also investigated. The contact load and the corresponding contact stress of the tooth pair changed due to changes the shape of the gear tooth geometry which in turn lead to change in the gear sliding wear. The effect of profile modification and face width crowning on sliding wear was studied by Mao [14]. The surface tooth wear on the profile modified gear tooth (tip relief and width modified) was lower than that of an unmodified gear tooth. The sliding wear on the tooth contact surface of a positive corrected gear was lesser than the negatively corrected gear. In  $S_o$  gears ( $x_1 = -x_2$ ), the maximum wheel teeth wear was 1.85 times faster than pinion teeth [15-17]. Some authors have developed a wear model to quantify the effects of surface roughness, specific film thickness misalignment, contact load, correction factor and slide to roll ratio on accumulated wear depth in gear contact surfaces. Surface roughness with lower value results in low stress concentration at both surface and subsurface of the contact region [18]. The gear misalignment might worsen the load distribution status and accelerate the sliding wear [19-20]. Prabhu Sekar and Sathish Kumar [21] determined the gear tooth strength, and wear depth on non-standard symmetric NCR gears through a mixed finite element and analytical approach. The non-standard symmetric spur gears have more tooth strength and wear resistance than standard symmetric spur gears.

In the available literature, very few studies deal with the improvement of gear performance by modifying the tooth shape. The gear tooth profile can be modified by changing the basic gear parameters or providing unequal circular tooth thickness at the respective pitch circle of the pinion and gear. Kapelevich [22] developed the gear tooth with asymmetric involute profiles through direct design approach. In asymmetric spur gear, the pressure angle at the pitch circle of coast and drive sides are different. He reported that the bending and contact strengths of the asymmetric spur gear were high when it was loaded at the high-pressure angle side than that of the low pressure angle side. The low and high-pressure angle sides are called as coast and drive sides of the asymmetric spur gear tooth. Importantly, Karpat et al. [23] determined the wear depth on NCR asymmetric gear with and without tip relief modification. Their findings showed that the tip relief modification reduced the wear depth in asymmetric spur gear tooth. The mathematical design procedure for generating the non-circular gear was demonstrated by Litvin et al [24]. Costopoulos and Spitas [25] developed a one-sided involute asymmetric gear tooth to improve the bending strength. Muni and Muthuveerappan [26] investigated the tooth bending stresses on asymmetric internal spur gear drives. Alipiev [27] developed a geometric design procedure for symmetric and asymmetric spur gears using realized potential method. This method was considered an appropriate one for gear drives with small number of teeth.

Many of the available research works on asymmetric spur gear deal with the methods for generation of asymmetric tooth and its full stress analysis computation. Apart from the bending and contact strengths, wear resistance should also be considered as an extra data variable to be taken into consideration in the optimum design for profile modifications. However, in all available earlier research studies, the tooth wear on direct designed HCR asymmetric spur gear have not been dealt with. Hence, this research work presents a much needed complete comparative analysis of gear performance (covering contact stresses, EHL film thickness, sliding distance, coefficient of friction, wear depth, power losses and efficiency) between the direct designed NCR and HCR asymmetric spur gear drives. Here, a methodology that combines a FEM based tooth contact model and Archard's wear estimation model is used to describe the determination of sliding wear on both direct designed NCR and HCR asymmetric spur gear pairs.

## 2 DIRECT DESIGN METHOD FOR SPUR GEAR

In the gear manufacturing industry, two different methods such as direct and conventional design methods are used to design a gear. A straight sided basic rack cutter with standard proportions is used to generate the pinion and gear in gear cutting process. The basic rack parameters such as addendum height, addendum height, pressure angle, tooth height, rack shift and rack tip radius are predefined and used as fixed input design parameters in the conventional design approach. However, in direct design method, the operating gear drive parameters such as speed ratio ( $i$ ), teeth number ( $z_p$ ), asymmetric factor ( $k$ ), module ( $m$ ), drive side contact ratio ( $\epsilon_d$ ) and top land thickness coefficient ( $L_a$ ) are predefined to develop the asymmetric tooth profile and then, the basic rack parameters are derived from the arrived configuration of asymmetric tooth profile. In direct design approach, an area of existence (AOE) is established to select a suitable design solution for pinion and gear. Hence, for user defined (customized) gears, the direct design method offers better design solutions than conventional gear design approach.

During the power transmission, one side of the gear tooth is loaded heavily for long time than the other side of the tooth. The asymmetric spur gear tooth is designed to enrich the performance of the loading side tooth geometry by diminishing the performance of the unloading side and the same is shown in Fig. 1. The asymmetric spur gear tooth is defined as one whose pressure angles on loading (drive) and unloading (coast) sides are different. The pressure angle at drive side involute is higher than the coast side involute and these two involute tooth profiles are generated from two different base circles.

The pressure angle at the base circle of the coast and drive sides ( $\alpha_{bc}$  and  $\alpha_{bd}$ ) are always equal to zero. From Fig. 1(a) and (b), the coast and drive side pressure angles ( $\nu_c$  and  $\nu_d$ ) at tip circle are defined by,

$$r_{\Delta} \cos \nu_c = r_a \cos \alpha_{ac} = r_{bc} \quad (1)$$

$$r_{\Delta} \cos \nu_d = r_a \cos \alpha_{ad} = r_{bd} \quad (2)$$

where,  $r_{bc}$  and  $r_{bd}$  are the base circle radii at coast and drive sides,  $r_{\Delta}$  is the radius at tip circle,  $\alpha_{ac}$  and  $\alpha_{ad}$  are the coast and drive side pressure angles at addendum circle and  $r_a$  is the radius at addendum circle. The ratio between the coast and drive side base circle radii is called asymmetric factor ( $k$ ). The asymmetric factor is equal to one ( $k=1$ ) for symmetric spur gear and it is greater than one ( $k>1$ ) for an asymmetric spur gear [22].

Dividing Eqs. (1) by (2), gives the asymmetric factor,

$$k = \frac{r_{bc}}{r_{bd}} = \frac{\cos \nu_c}{\cos \nu_d} = \frac{\cos \alpha_{ac}}{\cos \alpha_{ad}} \quad (3)$$

The top land tooth thickness coefficient ( $L_a$ ) is defined as the ratio of tooth thickness at addendum circle ( $t_a$ ) to the drive side base circle diameter ( $d_{bd}=2r_{bd}$ ). The value of top land tooth thickness coefficient should be chosen within  $(0.25 - 0.4) / z$  range, where  $z$  is teeth number [22]. The top land tooth thickness coefficient ( $L_a$ ) is defined by,

$$L_a = \frac{\left( \text{inv } \nu_d + \text{inv} \left( \cos^{-1} \left( k \cos \nu_d \right) \right) - \text{inv } \alpha_{ad} - \text{inv } \alpha_{ac} \right)}{2 \cos \alpha_{ad}} \quad (4)$$

where  $r_{bd} = r_a \cos \alpha_{ad}$ , involute function  $inv v_d = \tan v_d - v_d$

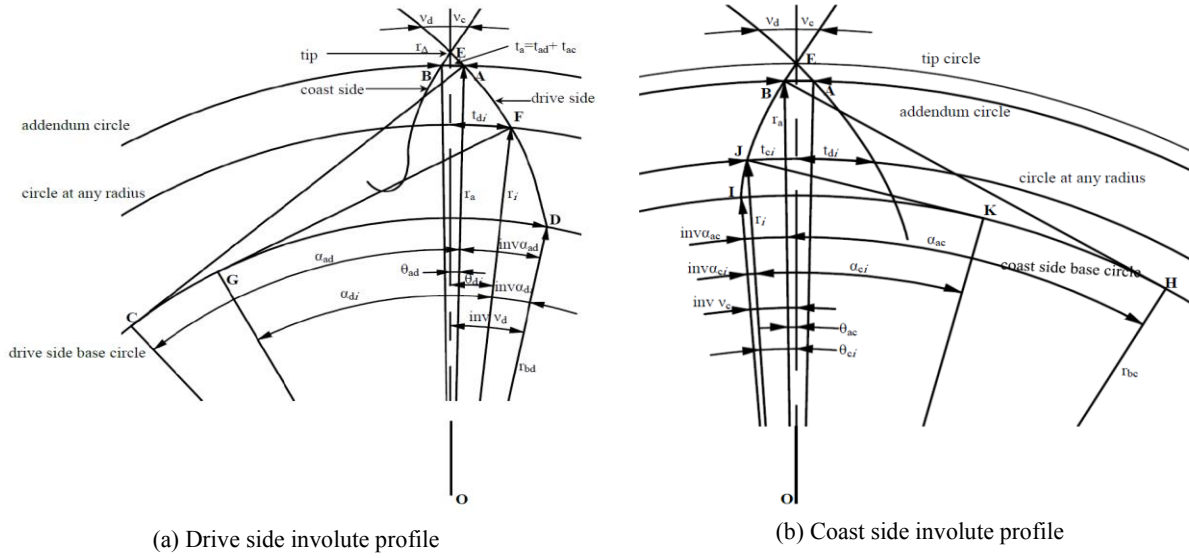


**Fig.1**  
Involute tooth profiles for asymmetric spur gear.

In backlash free gear drive, the algebraic sum of tooth thickness of gear and pinion at pitch circles is called as circular pitch ( $t_{og}=0.5 \pi m$  and  $t_{op}=0.5\pi m$ ) and it is given as,

$$t_{op} = t_{og} = \pi m$$

The pinion and gear tooth thickness at the respective pitch circle ( $t_{op}$  and  $t_{og}$ ) are defined by,

$$t_{op} = r_{op} (inv v_{dp} + inv v_{cp} - inv \alpha_{od} - inv \alpha_{oc}) = 0.5 \pi m \tag{5}$$

$$t_{og} = r_{og} (inv v_{dg} + inv v_{cg} - inv \alpha_{od} - inv \alpha_{oc}) = 0.5 \pi m \tag{6}$$

The involute function is defined by

$$inv \alpha_{od} + inv \alpha_{oc} = \frac{\left( (inv v_{dp} + inv v_{cp}) + i (inv v_{dg} + inv v_{cg}) - \frac{2\pi}{z_p} \right)}{1 + i} \tag{7}$$

Contact ratio plays a major role to ensure the continuous and non-jerky motion of the gear drive during the power transmission. Theoretically, it is defined as a measure average number of teeth pairs in contact in a mesh cycle. The contact ratio is less than two in NCR asymmetric spur gears ( $1 < \epsilon_d < 2$ ), whereas, this value is more than two in HCR asymmetric spur gears ( $\epsilon_d > 2$ ). Three pairs of contact in HCR asymmetric gear drive are shown in Fig. 2. During the transmission, for a period of time three pairs of teeth share the full load and for the remaining time only two pairs share the full normal load. The typical loading points of the HCR gear are LPTC, FLPDTC, FHPDTC, SLPDTC, SHPDTC, HPTC which are denoted as A, B, C, D, E and F respectively. The AB, CD and EF are the triple pair contact regions whereas the remaining BC and DE are the double pair contact regions. The corresponding radial distances are given by Eqs. (8) to (13).

$$r_{HPTC} = r_{ap} \tag{8}$$

$$r_{SHPDTC} = \sqrt{\left(\sqrt{r_{ap}^2 - r_{bdp}^2} - AF + 2p_{bd}\right)^2 + r_{bdp}^2} \quad (9)$$

$$r_{SLPDTC} = \sqrt{\left(\sqrt{r_{ap}^2 - r_{bdp}^2} - p_{bd}\right)^2 + r_{bdp}^2} \quad (10)$$

$$r_{FHPDTC} = \sqrt{\left(\sqrt{r_{ap}^2 - r_{bdp}^2} - AF + p_{bd}\right)^2 + r_{bdp}^2} \quad (11)$$

$$r_{FLPDTC} = \sqrt{\left(\sqrt{r_{ap}^2 - r_{bdp}^2} - 2p_{bd}\right)^2 + r_{bdp}^2} \quad (12)$$

$$r_{LPTC} = \sqrt{\left(\sqrt{r_{ap}^2 - r_{bdp}^2} - AF\right)^2 + r_{bdp}^2} \quad (13)$$

where, AF is length of path of contact,  $p_{bd}$  ( $p_{bd} = \pi m \cos \alpha_{od}$ ) is a base pitch at drive side,  $r_{ag}$  and  $r_{ap}$  are the radii at addendum circle for gear and pinion. HPTC – Highest point of tooth contact, SHPDTC – Second highest point of double tooth contact, SLPDTC – Second lowest point of double tooth contact, FHPDTC – First highest point of double tooth contact, FLPDTC – First lowest point of double tooth contact and LPTC- Lowest point of tooth contact.

In higher contact ratio gear drive, as the contact ratio is better it will give performance with lesser noise, impact and vibration. Nowadays, the HCR spur gear is preferred more than the helical gear due to the absence of axial thrust force. The drive side contact ratio of the asymmetric spur gear is given as [34],

$$\text{Contact ratio } (\varepsilon_d) = \frac{\text{Length of path of contact (AF)}}{\text{Base pitch } (p_{bd})}$$

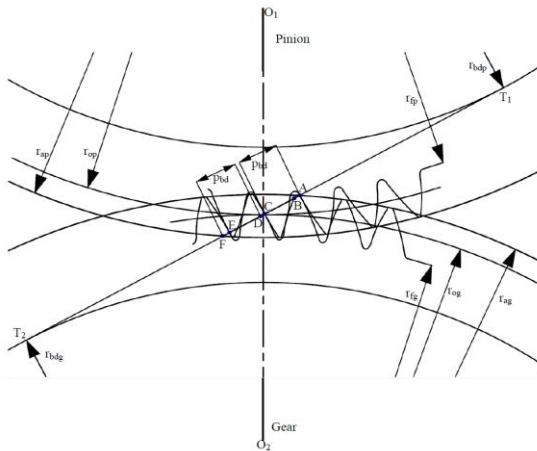


**Fig.2**  
Schematic for three pairs contact.

The drive side contact ratio for asymmetric spur gear is defined in terms of addendum pressure angle of the gear and pinion ( $\alpha_{adg}$  and  $\alpha_{adp}$ ) as,

$$\varepsilon_d = \frac{z_p}{2\pi} \left( \tan \alpha_{adp} + i \tan \alpha_{adg} \right) - (1+i) \tan \alpha_{od} \quad (14)$$

To maintain interference free contact, coast and drive side pressure angles at lowest point of contact should be greater or equal to zero [22]. The drive side pressure angle at LPTC for pinion ( $\alpha_{lpdp}$ )

$$\tan \alpha_{lpdp} = (1+i) \tan \alpha_{od} - i \tan \alpha_{adg} \tag{15}$$

where speed ratio  $i = r_{bdg} / r_{bdp}$

The drive side pressure angle at LPTC for gear ( $\alpha_{lpdg}$ )

$$\tan \alpha_{lpdg} = \frac{1+i}{i} \tan \alpha_{od} - \frac{\tan \alpha_{adp}}{i} \tag{16}$$

Similarly, the coast side pressure angles at LPTC for gear and pinion are expressed as,

$$\tan \alpha_{lpcg} = \frac{1+i}{i} \tan \alpha_{oc} - \frac{\tan \alpha_{acp}}{i} \tag{17}$$

$$\tan \alpha_{lpcp} = (1+i) \tan \alpha_{oc} - i \tan \alpha_{acg} \tag{18}$$

### 3 AREA OF EXISTENCE DIAGRAM FOR HIGHER CONTACT RATIO ASYMMETRIC SPUR GEARS

For given input parameters such as top land tooth thickness coefficient for gear and pinion ( $L_{ag}$  and  $L_{ap}$ ), gear ratio ( $i$ ), drive side contact ratio ( $\epsilon_d$ ), number of teeth in pinion ( $z_p$ ) asymmetric factor ( $k$ ) and module ( $m$ ), the addendum pressure angles for gear and pinion at drive side ( $\alpha_{adg}$  and  $\alpha_{adp}$ ) are determined using the derived equations (Eqs. (3), (4), (7), (14), (17) and (18)). The isograms  $A_i$ ,  $B_i$  and  $C_i$  are drawn in  $\alpha_{adp} - \alpha_{adg}$  coordinates and the enclosed region between these isograms is called as area of existence (AOE- shaded region in Fig. 3) from which a suitable design solution can be selected for the gear and pinion. The AOE diagram for higher contact ratio asymmetric spur gear has been developed by fixing the input parameters viz.  $i=1$ ,  $k=1.1$ ,  $m=1$ ,  $z_p=80$ ,  $L_{ap}=0.25/z_p$  and  $L_{ag}$

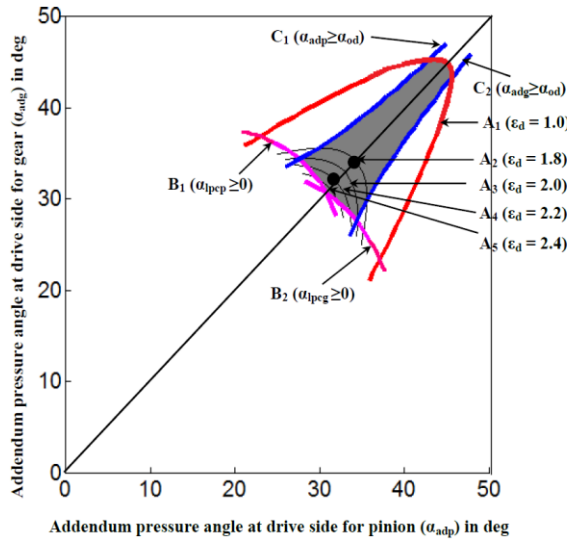


**Fig.3**  
AOE diagram for HCR asymmetric spur gear (For  $k=1.1$ ,  $m=1$ ,  $z_p=80$ ,  $L_{ap}=0.25/z_p$  and  $L_{ag}=0.25/z_g$ ).

From the area of existence diagram, the pressure angles at addendum circle for gear and pinion ( $\alpha_{adg}$  and  $\alpha_{adp}$ ) can be chosen anywhere within the shaded area to design the rack cutters for a required contact ratio. Fig. 4 shows the rack cutter for direct designed asymmetric spur gear that is used to make the involute and trochoidal tooth geometry.

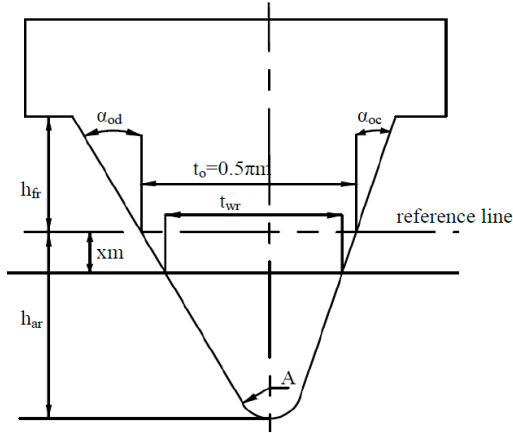


**Fig.4**  
Asymmetric rack cutter.

The rack tip radius ( $A$ ) is given as, [28]

$$A = \frac{0.5\pi m - h_{ar} (\tan \alpha_{od} + \tan \alpha_{oc})}{\left( \frac{1}{\cos \alpha_{od}} + \frac{1}{\cos \alpha_{oc}} \right) - (\tan \alpha_{od} + \tan \alpha_{oc})} \quad (19)$$

#### 4 GENERATION OF ASYMMETRIC INVOLUTE TOOTH PROFILE ON DRIVE AND COAST SIDES

The special plane curves such as involute and trochoidal curves are commonly used to form the symmetric and asymmetric gear tooth. Matlab code has been developed to determine the series coordinate points on the involute profiles for asymmetric tooth through Eqns. 32-35 and these series points are connected using special curves.

From Fig. 1(a and b), the angles  $\theta_{di}$  and  $\theta_{ci}$  at any radius ( $r_i$ ) on drive and coast side involute curves are calculated by,

$$\theta_{di} = \frac{t_{ad}}{r_a} + \text{inv } \alpha_{ad} - \text{inv } \alpha_{di} \quad (20)$$

$$\theta_{ci} = \frac{t_{ac}}{r_a} + \text{inv } \alpha_{ac} - \text{inv } \alpha_{ci} \quad (21)$$

The coordinates of the drive and coast side involute profiles at any circle are defined by:

Drive side coordinates

$$x_{di} = r_i \sin \theta_{di} \quad (22)$$

$$y_{di} = r_i \cos \theta_{di} \quad (23)$$

Coast side coordinates

$$x_{ci} = r_i \sin \theta_{ci} \quad (24)$$

$$y_{ci} = r_i \cos \theta_{ci} \quad (25)$$

### 5 DETERMINATION OF WEAR DEPTH IN HCR ASYMMETRIC GEARS

Gear pairs move with the combination of sliding and rolling motion during the period of contact. Sliding wear occurs at the teeth contact surfaces due to the rubbing action between the two mating gears. According to Archard's wear theory [11], wear depth at drive side ( $h_d$ ) is defined as follows:

$$h_d = \int_0^s K_w \sigma_H ds \tag{26}$$

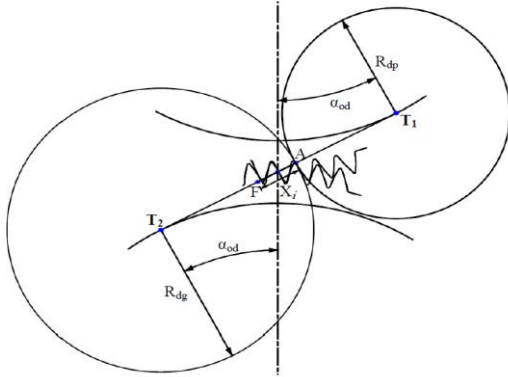


**Fig.5**  
Contact between two solid cylinders.

where,  $\sigma_H$  is contact pressure at the contact surface in MPa,  $s$ -sliding distance in m and Coefficient of wear  $K_w = 5 \times 10^{-16} \text{ m}^2/\text{N}$  [13]. The wear resistance of the gear tooth is a function of contact load, contact pressure, sliding velocity, sliding distance, surface condition and lubrications. The tooth load ( $F_i$ ) and the corresponding contact pressure ( $(\sigma_H)_i$ ) at any point ( $i$ ) along the line action are determined through finite element tooth contact analysis. The HCR asymmetric gear contact condition is modeled as a pair of two cylinders in contact and the same is shown in Fig. 5.

The Hertzian half-contact width ( $a_{di}$ ) is determined by, [29]

$$a_{di} = \sqrt{\frac{4F_i}{\pi b} \frac{\frac{1-\chi_p^2}{E_p} + \frac{1-\chi_g^2}{E_g}}{\frac{1}{(R_{dp})_i} + \frac{1}{(R_{dg})_i}}} \tag{27}$$

The radii of the contact cylinders at any contact point are defined as, [13] (Fig. 5)

$$(R_{dg})_i = r_{og} \sin \theta_{od} + X_i \tag{28}$$

$$(R_{dp})_i = r_{op} \sin \theta_{od} - X_i \tag{29}$$

where,  $\chi_g, \chi_p$  are the Poisson's ratio of the gear and pinion materials.  $E_g, E_p$  are the modulus of elasticity,  $X_i$  is the distance between any contact point ( $i$ ) and the pitch point. The sliding distance of the asymmetric gear and pinion at any contact points are,

$$(s_{dg})_i = 2a_{di} \left( \frac{(v_{dg})_i - (v_{dp})_i}{(v_{dg})_i} \right) \tag{30}$$



$$(s_{dp})_i = 2a_{di} \left( \frac{(v_{dp})_i - (v_{dg})_i}{(v_{dp})_i} \right) \quad (31)$$

where,  $v_{dg}$  and  $v_{dp}$  are velocities of the gear and pinion which are evaluated using the relations given below,

$$(v_{dg})_i = \omega_g (R_{dg})_i \quad (32)$$

$$(v_{dp})_i = \omega_p (R_{dp})_i \quad (33)$$

The sliding and rolling velocities respectively are defined as,

$$(V_{ds})_i = \left| (v_{dp})_i - (v_{dg})_i \right| \quad (34)$$

$$(V_{dR})_i = \left| (v_{dp})_i + (v_{dg})_i \right| \quad (35)$$

The entraining velocity ( $V_{de}$ ) and slide to roll ratio (SR) are determined by using the following relations,

$$(V_{de})_i = \frac{1}{2} \left| (v_{dp})_i + (v_{dg})_i \right| \quad (36)$$

$$(SR)_{di} = \frac{(V_{ds})_i}{(V_{de})_i} \quad (37)$$

The life of the gear drive is also affected by the elasto hydrodynamic lubricant (EHL) film thickness. Hamrock and Dowson [31] were proposed a relation to calculate the EHL film thickness ( $\phi_L$ ) which is given as:

$$(\phi_L)_i = 2.69 U_i^{0.67} G^{0.53} W_i^{-0.067} (1 - 0.61e^{-0.73K}) R_i \quad (38)$$

The non-dimensional speed factor ( $U_i$ ) is defined as,

$$U_i = \frac{(V_{de})_i \gamma_o}{E' R_i} \quad (39)$$

Equivalent radius of curvature at any contact position ( $R_i$ ) is given by,

$$R_i = \frac{(R_{dp})_i (R_{dg})_i}{(R_{dp})_i + (R_{dg})_i} \quad (40)$$

In which

$$E' = \frac{2}{\left( \frac{1 - \chi_p^2}{E_p} + \frac{1 - \chi_g^2}{E_g} \right)} \quad (41)$$

Material constant ( $G$ ) is defined as the product of pressure viscosity coefficient ( $\rho$ ) and  $E'$  and it is written as,

$$G = E' \rho \tag{42}$$

The load factor  $W_i$  is expressed as,

$$W_i = \frac{F_i}{E' R_i^2} \tag{43}$$

where, coefficient of ellipticity  $K = 12$  [32], dynamic viscosity  $\gamma_o = 0.0065$  Pas and pressure viscosity coefficient ( $\rho$ ) =  $1.2773 \times 10^{-8}$  1/Pa [30].

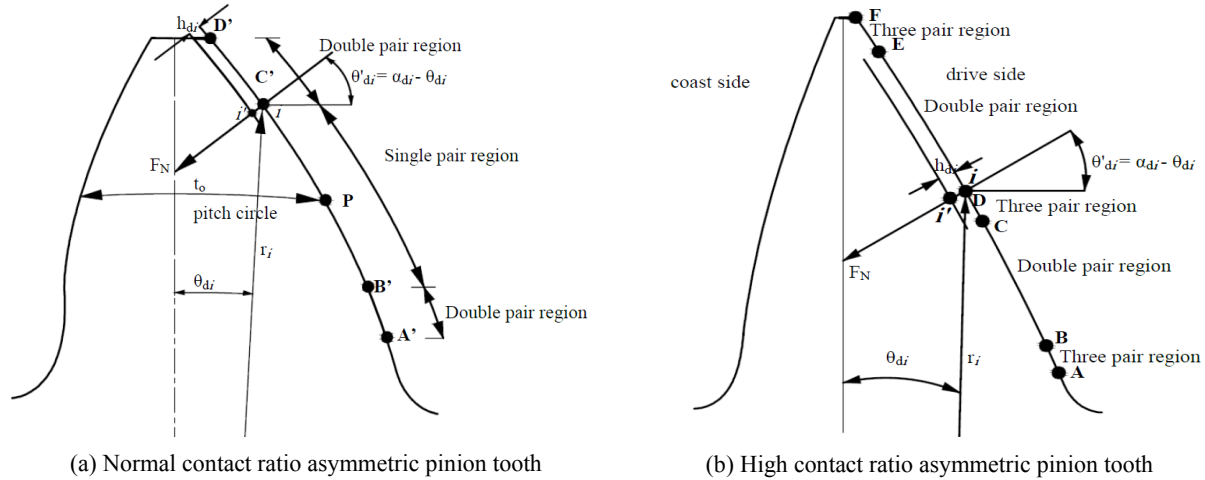


**Fig.6**  
Representation of worn out tooth profile for NCR and HCR pinion teeth.

Frictional force is a force created by the teeth pair surfaces contacting and sliding against each other which is affected by the surface finish and the amount of force pushing them together. The coefficient of friction between the teeth contact pair can be determined by using the model proposed by Xu [30] which includes parameters like load share, contact pressure, surface roughness, dynamic viscosity of lubricant, radius of curvature and entrainment velocity.

Equation for calculating the coefficient of friction is given as,

$$\mu_i = e^{f(SR_{di}, (\sigma_H)_i, \gamma_o, s)} (\sigma_H)_i^{c_2} |SR_{di}|^{c_3} (V_{de})_i^{c_6} \gamma_o^{c_7} R_i^{c_8} \tag{44}$$

In which

$$f(SR_{di}, (\sigma_H)_i, \gamma_o, s) = c_1 + c_4 |SR_{di}| (\sigma_H)_i \log \gamma_o + c_5 e^{-|SR_{di}| ((\sigma_H)_i \log \gamma_o)} + c_9 e^s \tag{45}$$

where, Surface roughness  $S = 0.1 \mu m$  [30], SR is the slide to roll ratio,  $c_i = -8.92, 1.03, 1.04, -0.35, 2.81, -0.10, 0.75, -0.39$  and  $0.62$  for  $i = 1$  to  $9$  respectively [30].

The accrued wear depth ( $h_{di}$ ) on drive side of the gear and pinion teeth surfaces for ‘n’ number of mesh cycles is calculated by, [13]

For gear,

$$h_{di,n} = h_{di,(n-1)} + K_w (\sigma_H)_i (S_{dg})_i \tag{46}$$

For pinion,

$$h_{di,n} = h_{di,(n-1)} + K_w (\sigma_H)_i (S_{dp})_i \quad (47)$$

Here, the determined values of contact pressure through FEM are substituted in Eqs. (46) and (47) and the accrued wear depth on the HCR asymmetric gear is calculated for 2000 mesh cycles. The HCR asymmetric pinion tooth surface is updated for every 250 mesh cycles. The schematic worn out tooth profile for NCR and HCR asymmetric tooth are shown in Fig. 6. The relations for evaluating the cartesian coordinates of the worn out pinion tooth profile are given as,

$$x'_{di} = x_{di} - h_{di} \cos \theta'_{di} \quad (48)$$

$$y'_{di} = y_{di} - h_{di} \sin \theta'_{di} \quad (49)$$

where,  $h_{di}$  is accumulated wear depth for 'n' no of cycles.

## 6 POWER LOSSES AND EFFICIENCY OF NCR AND HCR SPUR GEARS

In general, the frictional power losses that occur in the gear box are classified into two groups, sliding power losses and rolling power losses. The tooth mesh frictional power loss in the gearing system is given as,

$$(P_{frictional})_i = (P_S)_i + (P_R)_i$$

The sliding power losses occur in the gear box during the meshing cycle which is mainly due to the relative sliding motion between the two contacting surfaces. The product of sliding frictional force  $(F_S)_i$  and sliding velocity  $(V_{ds})_i$  at any instantaneous contact point ( $i$ ) gives the sliding power losses. The instantaneous sliding power loss  $(P_S)_i$  is given by,

$$(P_S)_i = (F_S)_i (V_{ds})_i \quad (50)$$

The sliding force developed at the contact surfaces is determined by,

$$\text{Sliding force } (F_S)_i = \mu_i F_i$$

where,  $\mu_i$  is the coefficient of friction and  $F_i$  is the load shared by a contact pair at any contact point  $i$ .

The hydrodynamic rolling (or pumping) loss is the power required to entrain and compress the lubricant to form a pressurized oil film, which separates the gear teeth. The model proposed by Anderson and Loewenthal [32] is used to estimate the rolling force at all instantaneous contact points along the line of action and it is given by,

$$\text{Rolling force } (F_R)_i = 9 \times 10^7 (\varphi_t)_i (\phi_L)_i b$$

The instantaneous rolling power loss  $(P_R)_i$  is expressed by,

$$\text{Rolling power loss } (P_R)_i = (F_R)_i (V_{dR})_i \quad (51)$$

where,  $\varphi_t$  is a thermal reduction factor which is calculated through a relation developed by Cheng [33].  $\phi_L$  – EHL film thickness,  $b$  – face width,  $V_{dR}$  – rolling velocity.

The algebraic summation of sliding and rolling power losses at any instantaneous contact point is equal to total power loss at the respective contact point and it is given as follows,

$$(TP_{int})_i = (P_S)_i + (P_R)_i$$

Simpson's one third numerical integration rule is used to determine the total power loss for one mesh cycle (A to D). The total mesh power loss is expressed by,

For NCR spur gear drives ( $1 < \varepsilon_d < 2$ ),

$$TP = 2 \int_A^B (TP_{int})_i dx + \int_B^C (TP_{int})_i dx + 2 \int_C^D (TP_{int})_i dx \quad (52)$$

For HCR spur gear drives ( $2 < \varepsilon_d < 3$ ),

$$TP = 3 \int_A^B (TP_{int})_i dx + 2 \int_B^C (TP_{int})_i dx + 3 \int_C^D (TP_{int})_i dx + 2 \int_D^E (TP_{int})_i dx + 3 \int_E^F (TP_{int})_i dx \quad (53)$$

Thus, the average total power loss for a mesh cycle is given as,

For NCR spur gear drives,

$$(TP)_{avg} = \frac{TP}{AD} \quad (54)$$

For HCR spur gear drives,

$$(TP)_{avg} = \frac{TP}{AF} \quad (55)$$

Finally, the mechanical efficiency of the NCR and HCR gearing system is expressed by,

$$\eta = 100 \left( \frac{P_{input} - (TP)_{avg}}{P_{input}} \right) \quad (56)$$

The input power is calculated using the following relation,

$$P_{input} = \frac{2\pi N_p T_{input}}{60} \quad (57)$$

The input torque ( $T_{input}$ ) is given as,

$$T_{input} = F_N r_{bdp}$$

where,  $F_N$  is a normal force and  $r_{bdp}$  is the base circle radius on drive side for pinion.

## 7 FINITE ELEMENT MODEL FOR HIGH CONTACT RATIO ASYMMETRIC SPUR GEAR

Many complex real time problems can be solved by FEM based analysis with reasonable accuracy. An accurate estimation of contact load, fillet stress, contact pressure and wear resistance is needed to design a gear for high performance applications. In FEM study, the proper selection of mesh element, mesh pattern, element size, number of elements and boundary conditions are required to predict a more accurate result than other methods. The gear parameters required to generate the HCR asymmetric gears are given in Table 1. The coordinates of the NCR and HCR asymmetric gear tooth profiles in coast and drive sides are determined using the procedure given in Section 2. The calculated coordinate points are imported into ANSYS to get the 2D asymmetric spur gear model (Fig. 7). ANSYS 12 is used to evaluate the contact pressure in the gear tooth. Finite element model of gear can be formulated either as plane stress or plane strain condition. If the ratio between the face width and thickness of the

tooth at pitch circle ( $b/t_o$ ) is more than five, plane strain condition is considered as controlling and if it is less than five, the other basis of plane stress condition is selected. An asymmetric spur gear with wide face width is taken in this FEM study. Hence, only a plane strain condition is considered for stress analysis. A triangular Plane 42 element is used for discretization of the tooth geometry. Contact element (CONTA 172) and Target element (TARG 169) are used to define the contact between gear and pinion. The inner hub region of the pinion is constrained in radial direction and a rotational torque ( $T=F_N \times r_{bdp}$ ) is applied in the tangential direction. In addition, the gear hub is restrained in both radial and tangential directions. As the fillet and contact regions are the critical ones in the gear tooth performance, a convergence study has been made for different element sizes at the fillet and contact regions. The contact and fillet regions are discretized with very fine size of elements (87,000 elements for one pair > convergence level) and other far field regions are meshed with coarse elements to minimize the solution time (Fig.7 (b)). This mesh refinement study has been made for every parametric study.

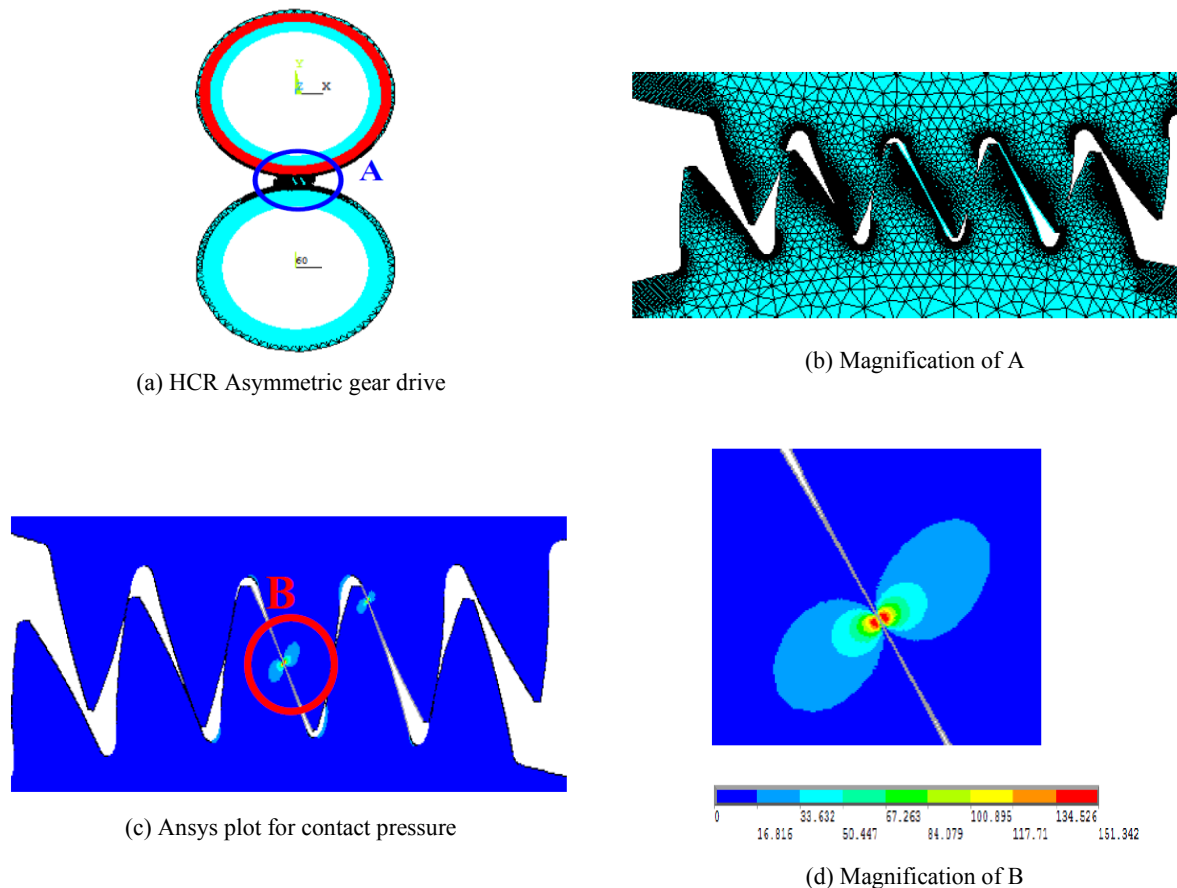


**Fig.7**

FE model for HCR asymmetric gear drive.

## 8 RESULTS AND DISCUSSION

### 8.1 Comparison of gear performance for direct designed NCR and HCR asymmetric spur gears

The addendum pressure angles for NCR (contact ratio  $\varepsilon_d=1.8$ ) and HCR ( $\varepsilon_d=2.2$ ) asymmetric pinion and gears are selected from the AOE diagram (Fig. 3). The asymmetric tooth profiles for NCR and HCR gears have been generated using matlab code. FEM study is used to estimate the load share and the respective contact pressure on direct designed NCR and HCR asymmetric spur gears. Apart from tooth load, contact stresses, wear resistance, mechanical power losses should also be considered as the extra data variables to be taken into consideration in the effective design of NCR and HCR asymmetric spur gears. The tooth load, load carrying capacity in contact, wear depth and the respective mechanical power losses are determined along the line action for given gear parameters (Table 1) and the same are shown in Fig. 8.

**Table 1**

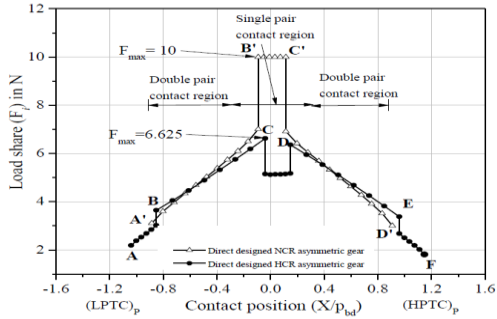
Gear parameters for direct designed NCR and HCR asymmetric spur gears.

S.No	Name of the gear parameter	NCR Symmetric gear	HCR Asymmetric gear
1.	Module ( $m$ ) in mm	1	1
2.	Gear ratio ( $i$ )	1	1
3.	Number teeth in pinion ( $z_p$ )	80	80
4.	Top land thickness coefficient ( $L_d$ )		
	For pinion	$0.25/z_p$	$0.25/z_p$
	For gear	$0.25/z_g$	$0.25/z_g$
5.	Asymmetric factor ( $k$ )	1.1	1.1
6.	Contact ratio	1.8	2.2
7.	Backup ratio ( $m_B$ )	2.22	2.22
8.	Total normal load ( $F_N$ ) in $N$	10	10
9.	Speed of pinion ( $N_p$ ) in $rpm$	150	150
10.	Modulus of elasticity ( $E$ ) in $MPa$	$2.1 \times 10^5$	$2.1 \times 10^5$
11.	Poisson's ratio ( $\chi$ )	0.3	0.3
12.	Width of the pinion and gear ( $b$ ) in $mm$	Unit width	Unit width
	Determined Parameters		Variable
1.	Addendum pressure angles at drive side for gear and pinion ( $\alpha_{adg}$ and $\alpha_{adp}$ ) degree	$34.78^\circ$	$31.97^\circ$
2.	Coast and drive side pressure angles at pitch circle ( $\alpha_{oc}$ and $\alpha_{od}$ ) degree	$\alpha_{oc} = 19.36^\circ$ $\alpha_{od} = 30.94^\circ$	$\alpha_{oc} = 14.2^\circ$ $\alpha_{od} = 28.20^\circ$
3.	Cutter tip radius ( $A$ ) $mm$	0.15702	0.23297
4.	Addendum modification factors ( $x_p$ and $x_g$ )	$x_p = 0.004, x_g = 0.004$	$x_p = 0.008, x_g = 0.008$

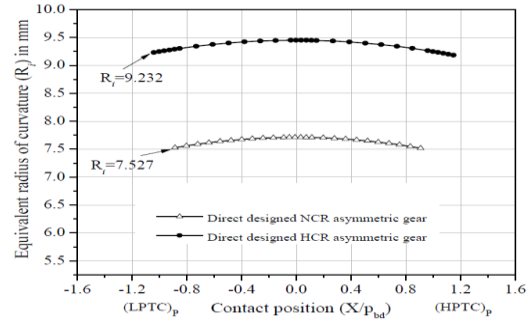
In NCR spur gear drives (Fig. 8 (a)), a contact begins at A' and ends at D'. During the transmission, the total normal load is shared by two pairs in the regions A'B', C'D' and only one pair shares the full normal load in the region B'C'. As the contact ratio increases beyond 2, the triple pair contacts exist, but these triple pair contacts are missing in NCR gear. In the higher contact ratio asymmetric spur gears, three pairs come in contact at the regions of AB, CD, EF and two pairs contact occur at BC and DE regions. Hence, the sum of the individual tooth load of each contact pair in the triple pair contact region is equal to the total normal load. A definite decrease in maximum load share is observed in asymmetric HCR gear (6.625 N at C) which is mainly due to the triple pair contact whereas it is almost equal to full load (10 N at B') due to a single pair contact in NCR asymmetric gear. Because of this reduced load share and an increased radius of curvature (Figs. 8 (a and b)), the highest contact pressure ( $154.25 < 212.84 MPa$ ) that develops in the direct designed HCR asymmetric gear is lesser than that in the NCR gear drive (Fig. 8 (c)). It is proved from this study that the contact strength of direct designed HCR asymmetric gear drive is higher than asymmetric NCR gear.

An increased EHL film thickness is noticed throughout the entire contacts in the HCR asymmetric gears due to the decrease in contact pressure at the respective contact positions (Fig. 8 (d)). A marginal reduction in velocity ratio at the beginning of the contact (point A) and a significant increase in velocity ratio at the end of the contact (point F) in HCR asymmetric spur gear are observed from Fig. 8 (e). The rise in radius of curvature leads to decrease in the velocity ratio ( $(1 - (v_{dg}/v_{dp}))$ ). Accordingly, the sliding distance, contact pressure and coefficient of friction decreases which leads to reduce the sliding wear in the tooth surface of the HCR asymmetric pinion (Figs. 8 (f, g and h)). It is also noted that in the HCR asymmetric gear, the maximum sliding wear occurs at the contact point B whereas in NCR asymmetric gear, it occurs at the beginning of the contact (point A' near root). There is no wear found at the pitch point due to pure rolling action (Fig. 8(g)). Hence, the direct designed HCR asymmetric gear alternative improves the wear resistance ultimately.

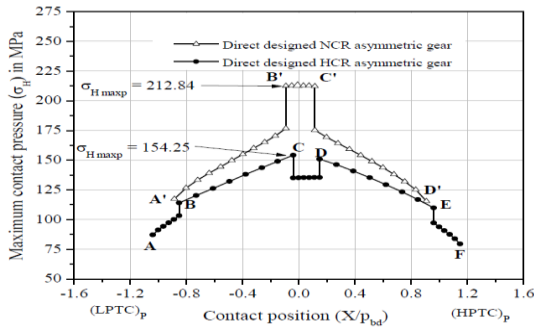
Even though the coefficient of friction is low, the sliding power losses is more in HCR asymmetric spur gear which is mainly due to the higher sliding velocity (Fig. 8 (i)). As the contact ratio increases, the sliding power loss increases due to the corresponding increases in sliding velocity, whereas the rolling power loss decreases due to the corresponding decrease in rolling velocity and contact load (Figs. 8 (i and j)). In HCR asymmetric spur gears, the amount of reduction in rolling power loss is more than that of rise in sliding power loss. A small amount of increase in mechanical efficiency is observed in the HCR spur gear drive (Fig. 8 (k)) which is mainly due to the decrease in total power loss (sum of rolling and sliding power losses along the path of contact) in the HCR asymmetric spur gear. Hence, HCR asymmetric spur gear drive improves the life of the spur gear drives.



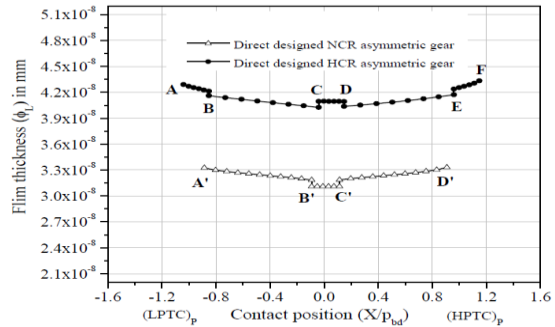
(a) Variation of load share along the line of contact



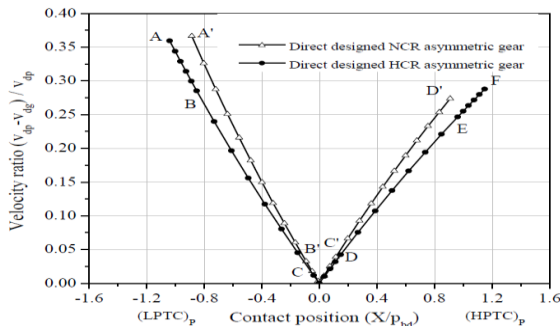
(b) Variation of equivalent radius of curvature along the line of contact



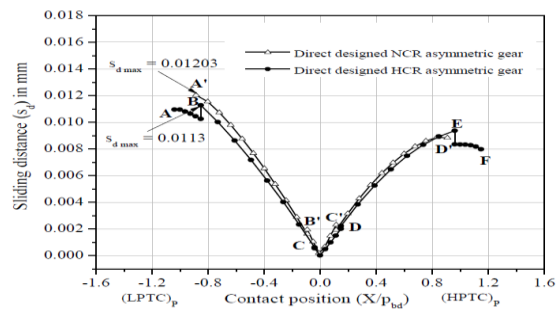
(c) Variation of contact pressure along the line of contact



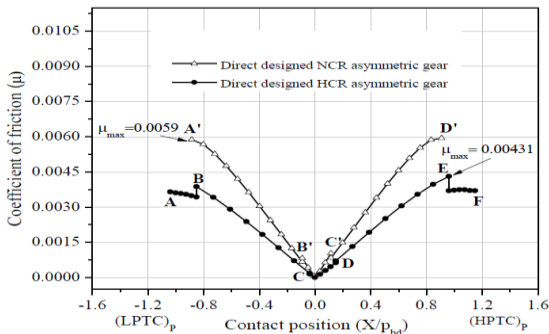
(d) Variation of film thickness along the line of contact



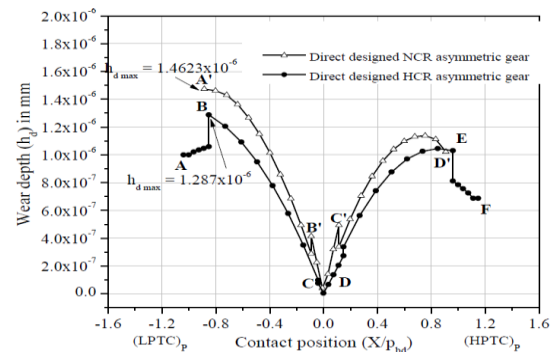
(e) Variation of velocity ratio along the line of contact



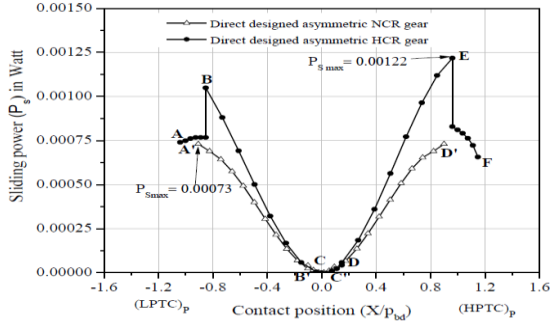
(f) Variation of sliding distance along the line of contact



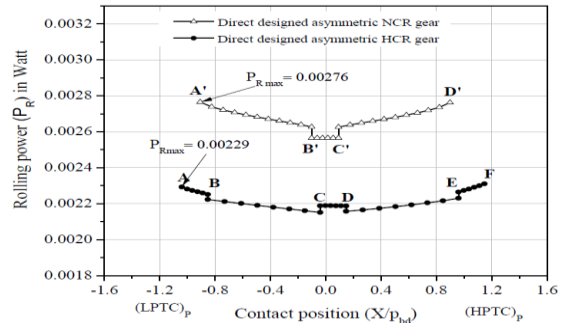
(g) Variation of coefficient of friction along the line of contact



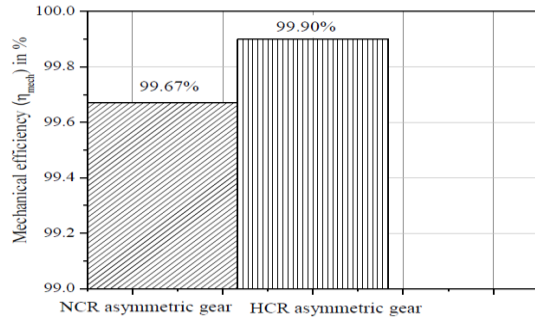
(h) Variation of wear depth along the line of contact



(i) Variation of sliding power loss along the line of contact



(j) Variation of rolling power loss along the line of contact



(k) Efficiency for NCR and HCR asymmetric spur gears

**Fig.8**  
Comparison of gear drive performance for NCR and HCR asymmetric spur gears.

## 9 CONCLUSIONS

In the present study, Normal and high contact ratio asymmetric spur gears have been developed through direct design approach. A detailed investigation on the load shares by a teeth contact pair, contact strength, sliding wear, power losses and the mechanical efficiency of direct designed NCR and HCR asymmetric spur gear drives has also been carried out using FE tooth contact model. The results found in this work are summarized as follows:

1. The direct design approach gives more number of design solutions for the given gear parameters than the conventional gear design method.
2. The maximum load share by a teeth contact pair is equal to the applied load ( $F_N=10\text{ N}$ ) in the direct designed NCR asymmetric gear, whereas it is almost equal to 66.25% ( $F_t= 6.625\text{ N}$ ) of the total normal load in direct designed HCR asymmetric gear. This reduced load share improves the contact load capacity of HCR asymmetric spur gears (Figs. 8 (a and c)).
3. In spur gears whether it is NCR or HCR, the amount of material loss is more in the flank region than that of the face region. The maximum sliding wear that occurs at the contact position B in flank region which is lower in the direct designed HCR asymmetric gear than that of the direct designed NCR asymmetric gear.
4. As the values of  $\epsilon_d$  increase, the mechanical efficiency increases slightly in the HCR asymmetric spur gear.

Through this study on contact strength, sliding tooth wear and power losses in the direct designed asymmetric gear and pinion, it is decided that an increase of contact ratio more than two, all result in enhancement of contact load capacity, wear resistance and mechanical efficiency. Thus, asymmetric HCR pinion and gear when properly designed, by making use of the changed parameters given above will result in enhanced gear performance in the HCR asymmetric spur gear drive.

## REFERENCES

- [1] Elkholy A.H., 1985, Tooth load sharing in high contact ratio spur gears, *Journal of Mechanisms, Transmissions, and Automation in Design* **107**: 11-16.
- [2] Tsai M.H., Tsai Y.C., 1997, Design of high contact ratio spur gears using quadratic parametric tooth profiles, *Mechanism and Machine Theory* **33**: 551-564.



- [3] Arafa M.H., Megahed M.M., 1999, Evaluation of spur gear mesh compliance using finite element method, *Proceedings of the Institution of Mechanical Engineers Part C, Journal of Mechanical Engineering Science* **213**: 569-579.
- [4] Saribay Z. B., 2012, Tooth geometry and bending stress analysis of conjugate meshing face-gear pairs, *Proceedings of the Institution of Mechanical Engineers Part C, Journal of Mechanical Engineering Science* **227**: 1302-1314.
- [5] Wang J., Howard I., 2005, Finite element analysis of high contact ratio spur gears in mesh, *Journal of Tribology* **127**: 469-483.
- [6] Li S., 2007, Effect of addendum on contact strength, bending strength and basic performance parameters of a pair of spur gears, *Mechanism and Machine Theory* **43**: 1557-1584.
- [7] Pedrero J., Vallejo I., Pleguezuelos M., 2007, Calculation of tooth bending strength and surface durability of high transverse contact ratio spur and helical gear drives, *Journal of Mechanical Design* **129**: 69-74.
- [8] Basan R., Franulović M., Križan B., 2008, Numerical model and procedure for determination of stresses in spur gears teeth flanks, *XII International Conference on Mechanical Engineering*, Bratislava, Slovakia.
- [9] Sivakumar P., Kopinath K., Sundaresh S., 2009, Performance evaluation of high-contact-ratio gearing for combat tracked vehicles – a case study, *Proceedings of the Institution of Mechanical Engineers Part D, Journal of Automobile Engineering* **224**: 631-643.
- [10] Thirumurugan R., Muthuveerappan G., 2011, Critical loading points for fillet and contact stresses in normal and high contact ratio spur gears based on load sharing ratio, *Mechanics Based Design of Structures and Machines* **39**: 118-141.
- [11] Archard A. F., 1953, Contact of rubbing flat surfaces, *Journal of Applied Physics* **24**: 981-988.
- [12] Wu S., Cheng H.S., 1993, Sliding wear calculation in spur gears, *ASME Journal of Tribology* **115**: 493-503.
- [13] Flodin A., Andersson S., 1997, Simulation of mild wear in spur gears, *Wear* **207**: 123-128.
- [14] Mao K., 2007, Gear Tooth contact analysis and its application in the reduction of fatigue wear, *Wear* **262**: 1281-1288.
- [15] Imrek H., Duzcukoglu H., 2007, Relation between wear and tooth width modification in spur gears, *Wear* **262**: 390-394.
- [16] Imrek H., Unuvar A., 2009, Investigation of influence of load and velocity on scoring of addendum modified gear tooth profiles, *Mechanism and Machine Theory* **44**: 938-948.
- [17] Chernets M., Chernets J., 2016, The simulation of Influence of engagement conditions and technological teeth correction on contact strength, wear and durability of cylindrical spur gear of electric locomotive, *Journal Engineering Tribology* **231**: 57-62.
- [18] Bergseth E., Sjoberg S., Bjorklund S., 2012, Influence of real surface topography on the contact area ratio in differently manufactured spur gears, *Tribology International* **56**: 72-80.
- [19] Parsa M., Akbarzadeh S., 2014, A new load sharing based approach to model mixed-lubrication contact of spur gears, *Journal Engineering Tribology* **228**: 1319-1329.
- [20] Zhang J., Liu X., 2015, Effects of misalignment on surface wear of spur gears, *Journal Engineering Tribology* **229**: 1145-1158.
- [21] Prabhu Sekar R., Sathish Kumar R., 2017, Enhancement of wear resistance on normal contact ratio spur gear pairs through non-standard gears, *Wear* **380-381**: 228-229.
- [22] Kapelevich A., 2000, Geometry and design of involute spur gears with asymmetric teeth, *Mechanism and Machine Theory* **35**: 117-130.
- [23] Karpat F., Osire S.E., 2008, Influence of tip relief modification on the wear of NCR spur gears with asymmetric teeth, *Tribology Transactions* **51**: 581-588.
- [24] Litvin F.L., Perez I.G., Fuentes A., Hayasaka K., 2008, Design and investigation of gear drives with non-circular gears applied for speed variation and generation function, *Computer Methods in Applied Mechanics and Engineering* **197**: 3783-3802.
- [25] Costopoulos T., Spitas V., 2009, Reduction of gear fillet stresses using one side asymmetric teeth, *Mechanism and Machine Theory* **44**: 1524-1534.
- [26] Muni D.V., Muthuveerappan G., 2009, A comprehensive study on the asymmetric internal spur gear drives through direct and conventional gear design, *Mechanics Based Design of Structures and Machines* **37**: 431-461.
- [27] Alipiev O., 2011, Geometric design of involute spur gear drives with symmetric and asymmetric teeth using the Realized Potential Method, *Mechanism and Machine Theory* **46**: 10-32.
- [28] Prabhu Sekar R., Muthuveerappan G., 2015, Estimation of tooth form factor for normal contact ratio asymmetric spur gear tooth, *Mechanism and Machine Theory* **90**: 187-218.
- [29] Maitra G.N., 2001, *Handbook of Gear Design*, Tata McGraw-Hill Pubns.
- [30] Xu H., Kahraman A., Anderson N., Maddock D., 2007, Prediction of mechanical efficiency of parallel-axis gear pairs, *Journal of Mechanical Design* **129**: 58-68.
- [31] Hamrock B.J., Dowson O., 1977, Isothermal elastohydrodynamic lubrication of point contacts, fully flooded results, *Journal of Lubrication Technology* **99**: 264-276.
- [32] Anderson N.E., Loewenthal S.H., 1980, Spur-Gear-System efficiency at part and full load, NASA TP-1622.
- [33] Cheng H.S., 1974, Prediction of film thickness and sliding frictional coefficient in elastohydrodynamic contacts, *Design Engineering Technology Conference, American Society of Mechanical Engineers*.
- [34] Maitra G.M., 1989, *Hand Book of Gear Design*, Tata McGraw Hill Publishing Company Limited, New Delhi.